International Journal of Engineering Research and Development
e-ISSN: 2278-067X, p-ISSN: 2278-800X, www.ijerd.com
Volume 8, Issue 5 (August 2013), PP. 54-63

A Novel Control Strategy to Reduce Transformer Inrush Currents by Series Voltage Sag Compensator

[1]venkatesh Dugyala, [2]ch.Nagalaxmi, [3]v.K.R.Mohan Rao
[1]PG Scholar, [2]Assistant Professor, [3]Associate Professor,
[1,2,3]Holy Mary Institute of Technology & Science

Abstract:- Inrush currents generated by unloaded power transformer often reduce power quality on the system. To improve this situation, this paper proposes an active inrush current compensator that is capable of reducing the inrush current effectively during startup mode. The proposed compensator is based on an inverter-based series compensator which is comprised of a single-phase inverter and series transformer. Voltage sags are very frequent events with energization of transformer or starting of large motors although their duration is very short. Hence, during voltage stabilizer mode, the existing series compensator is controlled by a voltage stabilizer controller and superimposes a compensating voltage on the inverter output whenever the load voltage deviate from the nominal value. This strategy is easier to implement because it requires no information of the transformer parameters, power on angle of circuit breaker and measurement of residual flux. Some simulations results show satisfactory performance of the proposed technique on both inrush current reduction and correcting voltage sags.

Keywords:- series compensator, transformer, inrush current, voltage sag.

I INTRODUCTION

TRANSFORMER energization at no load may result in a very high inrush current. The peak value of the inrush current is a function of the switching instant of the terminal voltage, the characteristics of the hysteresis curve (residual and saturation fluxes), the primary winding resistance, and the inherent primary winding air-core inductance. Inrush currents are originated by the high saturation of the iron core during switching in. Excellent physical explanations of the phenomenon can be found in [1] and [2]. The driving force of the inrush current is the voltage applied to the primary of the transformer. The voltage may drive the flux to build up to a maximum theoretical value of twice the steady-state flux plus any residual flux. This super-saturation of the core may lead to an inrush current hundreds of times larger than the normal excitation current and many times larger than the rated current.

There are three negative side effects of inrush currents: 1) the protective devices for overloads and internal faults may falsely operate and disconnect the transformer. References [3]–[11] are examples of the available techniques for relays to distinguish between faults and inrush currents used to reduce the number of undesirable trips; 2) the windings are exposed to mechanical stresses that can damage the transformer [12]–[14]; and 3) power-quality problems may arise: high resonant harmonic overvoltages [15] and voltage sags [16].

In an electric distribution network, when a feeder is energized following maintenance work, many parallel-connected network transformers draw inrush currents simultaneously. The purpose of this paper is to demagnetize "network transformers" [17], which are connected differently from (radial) "distribution transformers" [18]. The load of a radial distribution transformer remains connected when the transformer or feeder is offline. Therefore, the power to the loads (customers) is lost. In contrast, in networked systems, the secondaries of all network transformers, of different HV feeders are tied to each other through the low-voltage network. Therefore, when a feeder breaker is open, the associated network protectors to the transformers open (effectively isolating the feeder; that means, all network transformers are left open-circuited). As a result, in secondary networks, all loads are automatically re-routed and no disruption is felt by the customers.

II. SYSTEM DESCRIPTION

As shown in Fig. 1, the voltage sag compensator consists of a three-phase voltage-source inverter (VSI) and a coupling transformer for serial connection. When the grid is normal, the compensator is bypassed by the thyristors for high operating efficiency. When voltage sags occur, the voltage sag compensator injects the required compensation voltage through the coupling transformer to protect critical loads from being interrupted. However, certain detection time (typically within 4.0 ms) is required by the sag compensator controller to identify the sag event [19]–[21]. And the load transformer is exposed to the deformed voltage from the sag occurrence to the moment when the compensator restores the load voltage. Albeit its short duration, the

deformed voltage causes magnetic flux deviation inside the load transformer, and the magnetic saturation may easily occur when the compensator restores the load voltage, and thus, results in the inrush current. The inrush current could trigger the overcurrent protection of the compensator and lead to compensation failure. Thus, this paper proposes an inrush mitigation technique by correcting the flux linkage offsets of the load transformer, and this technique can be seamlessly integrated with the state-feedback controller of the compensator.

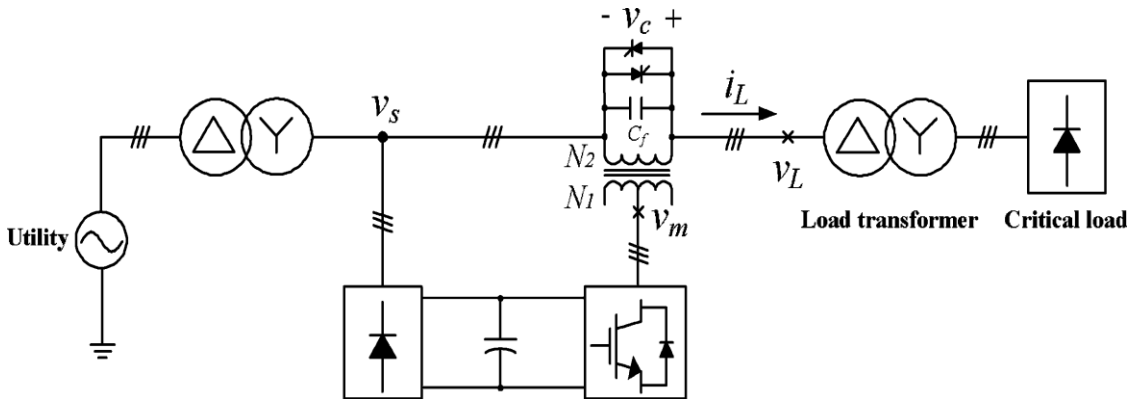

Fig.1 Simplified one-line diagram of the offline series voltage sag compensator

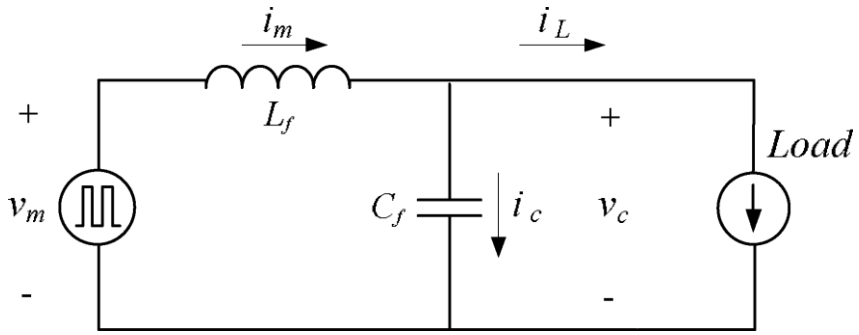

Fig.2 Per-phase equivalent circuit of the series voltage sag compensator.

The dynamics of the sag compensator will be described. The proposed inrush mitigation technique and its integration with the voltage and current closed-loop controls are also presented.

A. Dynamics of the Sag Compensator

The dynamics of the sag compensator can be represented by an equivalent circuit in Fig. 2. Generally, the sag compensator is rated for compensating all three-phase voltages down to 50% of nominal grid voltage. The coupling transformer is capable of electrical isolation or boosting the compensation voltage. In the proposed system, the turns ratio of the coupling transformer is set on unitary ($N1$:$N2$ = 1:1) to provide the maximum compensation voltage of the 50% of nominal value. Moreover, the leakage inductor of the coupling transformer is used as the filter inductor *Lf* and is combined with the filter capacitor *Cf* installed in the secondary winding of the coupling transformer to suppress pulse width modulated (PWM) ripples of the inverter output voltage v*m*. The dynamics equations are expressed as follows:

$$L_f \frac{d}{dt}\begin{bmatrix} i_{ma} \\ i_{mb} \\ i_{mc} \end{bmatrix} = \begin{bmatrix} v_{ma} \\ v_{mb} \\ v_{mc} \end{bmatrix} - \begin{bmatrix} v_{ca} \\ v_{cb} \\ v_{cc} \end{bmatrix} \qquad (1)$$

$$C_f \frac{d}{dt}\begin{bmatrix} v_{ca} \\ v_{cb} \\ v_{cc} \end{bmatrix} = \begin{bmatrix} i_{ma} \\ i_{mb} \\ i_{mc} \end{bmatrix} - \begin{bmatrix} i_{La} \\ i_{Lb} \\ i_{Lc} \end{bmatrix} \qquad (2)$$

Where $[v_{ma}\ v_{mb}\ v_{mc}]T$ is the inverter output voltage, $[i_{ma}\ i_{mb}\ i_{mc}]^T$ is the filter inductor current, $[v_{ca}\ v_{cb}\ v_{cc}]^T$ is the compensation voltage, and $[i_{La}\ i_{Lb}\ i_{Lc}]^T$ is the load current. Equations (1) and (2) are transformed into the synchronous reference frame as the following

$$\frac{d}{dt}\begin{bmatrix} i_{mq}^e \\ i_{md}^e \end{bmatrix} = \begin{bmatrix} 0 & -\omega \\ \omega & 0 \end{bmatrix}\begin{bmatrix} i_{mq}^e \\ i_{md}^e \end{bmatrix} + \frac{1}{L_f}\begin{bmatrix} v_{mq}^e \\ v_{md}^e \end{bmatrix} - \frac{1}{L_f}\begin{bmatrix} v_{cq}^e \\ v_{cd}^e \end{bmatrix} \tag{3}$$

$$\frac{d}{dt}\begin{bmatrix} v_{cq}^e \\ v_{cd}^e \end{bmatrix} = \begin{bmatrix} 0 & -\omega \\ \omega & 0 \end{bmatrix}\begin{bmatrix} v_{cq}^e \\ v_{cd}^e \end{bmatrix} + \frac{1}{C_f}\begin{bmatrix} i_{mq}^e \\ i_{md}^e \end{bmatrix} - \frac{1}{C_f}\begin{bmatrix} i_{Lq}^e \\ i_{Ld}^e \end{bmatrix} \tag{4}$$

where superscript "e" indicates the synchronous reference frame representation of this variable and ω is the angular frequency of the utility grid. Equations (3) and (4) show the cross-coupling terms between the compensation voltage and the filter inductor current. The block diagram of the physical circuit dynamics are illustrated in the right-hand side of Fig. 3.

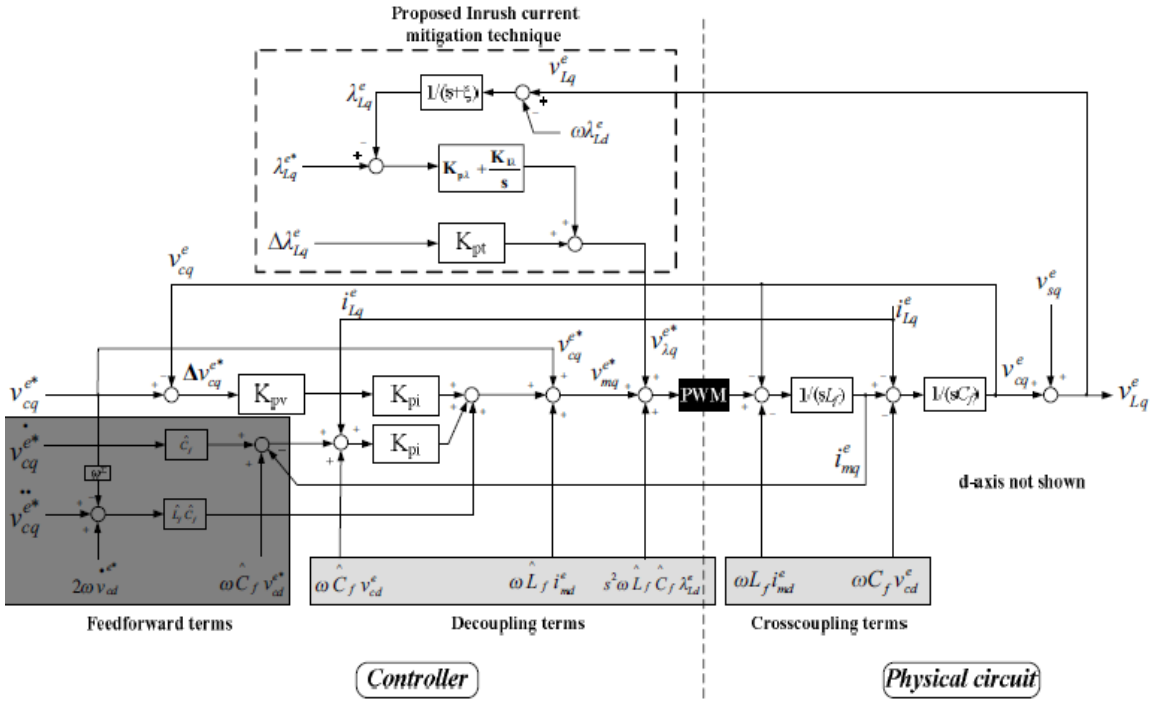

Fig.3 Block diagram of the proposed inrush current mitigation technique with the state-feedback control.

B. Voltage and Current Closed-Loop Controls

Fig. 3 shows the block diagram of the proposed control method. Note that the *d*-axis controller is not shown for simplicity. The block diagram consists of the full state-feedback controller and the proposed inrush current mitigation technique. The feedback control, feed forward control, and decoupling control are explained as follows.

1) Feedback Control: The feedback control is to improve the precision of the compensation voltage, the disturbance rejection capability, and the robustness against parameter variations. As shown in Fig. 3, the capacitor voltage v_{cq}^e and the inductor current i_{mq}^e are handled by the outer-loop voltage control and the inner-loop current control, respectively. The voltage control is implemented by a proportional gain K_{pv} with a voltage command v_{cq}^{e*} produced by the voltage sag compensation scheme. The current control also consists of a proportional control gain K_{pi} to accomplish fast current tracking.

2) Feedforward Control: To improve the dynamic response of the voltage sag compensator, the feedforward control is added to the voltage controller to compensate the load voltage immediately when voltage sag occurs. The feedforward voltage command can be calculated by combining the compensation voltage and the voltage drop across the filter inductor L_f.

3) Decoupling Control: The cross-coupling terms are the result of the synchronous reference frame transformation, as in (3) and (4). The controller utilizes the decoupling terms to negate the cross coupling and

reduce the nterferences between the *d–q* axes. Fig. 3 shows that the decoupling terms can be accomplished by the filter capacitor voltage v_{cq}^{e} the filter inductor current i_{mq}^{e} , and the estimated values of the filter capacitor and the filter inductor.

III. TRANSFORMER INRUSH PHENOMENON

The most severe case of magnetizing inrush current results from transformer energization. In this case there is a very large change in excitation voltage applied to the core. For three phase transformers, each phase will experience different peak values of inrush current due to the impact of the voltage angle at time of switching. The value of the transformer inrush current is a function of various factors, such as the switching angle of the terminal voltage, the remanent flux of the core, the transformer design, the power system impedance, and others. Holcomb proposes an improved analytical equation for the inrush current:

$$i(t) = \frac{\sqrt{2}U}{\sqrt{R_W^2 + \omega^2 . L_{\text{air-core}}^2}} \cdot \left(\sin(\omega t\_\phi) \_ e^{-\frac{R_W}{L_{\text{air-core}}}(t - t_s)} \sin(\omega t_s\_\phi) \right) \quad (5)$$

$$\phi = \tan^{-1} \frac{\omega . L_{\text{air-core}}}{R_W} \quad (6)$$

Where U is the applied voltage; R_w is the winding resistance; $Lair_{\text{-core}}$ is the air-core inductance of winding; and t_s is the time when the core begins to saturate (B (t) > Bs). It is assumed that the inrush current is different from zero only between t_s and t_0 where t_0 is the time when the inrush current reaches zero at each cycle. The air-core inductance $L_{\text{air-core}}$ of a winding can be calculated as:

$$L_{\text{air-core}} = \mu_0 . N_{HW}^2 . \frac{A_{HW}}{h} \quad (7)$$

Where, $h_{\text{eq-HV}}$ being the equivalent height of the winding including fringing effects. The equivalent height is obtained by dividing the winding height by the Rogowski factor k_R(< 1.0) [22]. This factor is usually determined empirically and is a function of the height, mean diameter, and radial width of a winding.

IV. INRUSH CURRENT MITIGATION TECHNIQUE

Flux linkage DC offset: The flux linkage is estimated by the measured line voltage. Figure 4 shows a single winding of the delta/wye three-phase load transformer which is installed in downstream of voltage sag compensator. The flux linkage of the phase a-b winding is expressed as

$$\lambda_{Lab}(t) = \int^{t} v_{Lab}(\tau) d\tau . \quad (8)$$

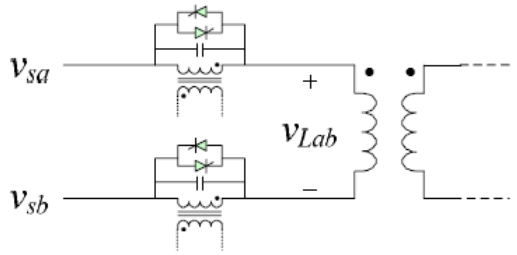

Fig.4 Connection diagram of the proposed system and delta/wye load transformer

Figure 5 illustrates the line-to-line voltage across the transformer winding and the resulting flux linkage from the sag occurrence to completion of voltage compensation. When voltage sags occurs (t=t sag), the controller detects the sagged voltage and injects the required compensation voltage at t=t detect.

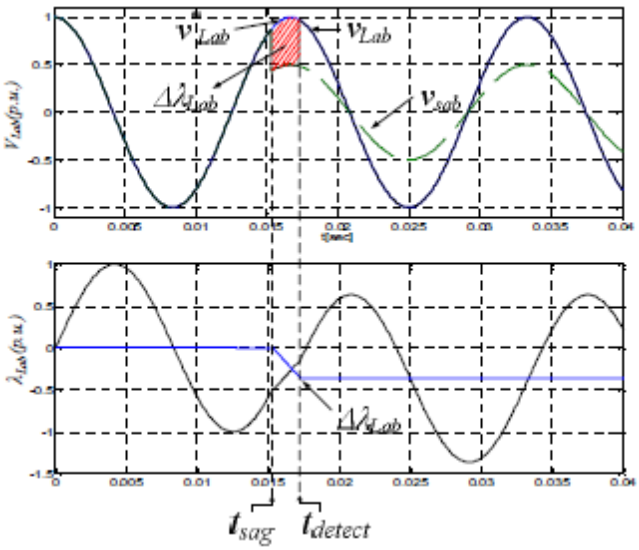

Fig.5 Transformer voltage and corresponding transient flux linkage

The flux linkage during the voltage compensation process can be express as following:

$$\lambda_{Lab}(t) = \lambda_{Lab}(t)|_{t=t_{\text{sag}}} + \int_{t_{\text{sag}}}^{t_{\text{action}}} v_{Lab}(\tau)\, d\tau + \int_{t_{\text{action}}}^{t} v^*_{Lab}(\tau)\, d\tau \qquad (9)$$

Assume the pre-fault load voltage is

$$v^*_{Lab}(t) = \hat{V}^*_{Lab} \sin(\omega t + \Phi^*_{Lab}) \qquad \forall t.$$

Where $\widehat{V^*_{\text{Lab}}}$ the magnitude of load voltage, ω is is the grid frequency, and $\emptyset^*_{\text{Lab}}$ is the phase angle. Thus, after the voltage compensation is completed, the flux linkage can be expressed as

$$\lambda_{Lab}(t) = \Delta\lambda_{Lab}(t)|_{t=t_{\text{action}}} + \frac{\hat{V}^*_{Lab}}{\omega} \sin\left(\omega t + \Phi^*_{Lab} - \frac{\pi}{2}\right) \quad \text{for} \quad t \geq t_{\text{action}} \qquad (10)$$

Where

$$\Delta\lambda_{Lab}(t)|_{t=t_{\text{action}}} = \int_{t_{\text{sag}}}^{t_{\text{action}}} (v_{Lab}(\tau) - v^*_{Lab}(\tau))\, d\tau. \qquad (11)$$

Equation (11) states that the sagged voltages cause the flux linkage DC offset Δλ Lab on the transformer windings, and its magnitude is dependent on the depth and the duration of sags. Severe voltage sag event can drive the DC offset exceeding the magnetic saturation knee and causes high inrush current. In practical saturation, the magnetic saturation knee is usually put on 1.10-1.15 p.u. of state-study flux linkage.

The Disturbance Rejection Capability: The stationary referenced frame control design causes a steady-state tracking error on the load voltage. Moreover, the control gain limitation constricts the compensator capability about disturbance rejection. The synchronous reference frame implementation of the proposed state feedback controller can effectively enhance the disturbance rejection capability compared to the stationary frame feedback controller design.

The proposed inrush current mitigation technique utilizes a flux linkage closed-loop control, and this feature elevates even further the disturbance rejection characteristics of the sag compensator for the fundamental frequency load current.

The disturbance rejection capability can be characterized by the transfer function between the compensator output voltage and the load current. Equation (12) and (13) show the disturbance rejection capability of the compensator under the conventional voltage-current state feedback controller and the proposed inrush current mitigation technique integrated with state feedback controller respectively.

$$\left\| \frac{i_{Lq}^{e}(s)}{v_{eq}^{e}(s)} \right\| = \frac{L_f C_f s^3 + K_{pi} C_f s^2 + (K_{pv}+1)s + K_{Iv}}{L_f s^2} \quad (12)$$

$$\left\| \frac{i_{Lq}^{e}(s)}{v_{eq}^{e}(s)} \right\| = \frac{L_f C_f s^4 + K_{pi} C_f s^3 + (K_{pv}+1)s^2 + K_{p\lambda} s + K_{I\lambda}}{L_f s^3}. \quad (13)$$

Note that three assumptions are made for simplicity, namely
1) cross-coupling terms in physical model has been decoupled by the controllers,
2) And the utility voltage is a voltage stiff,
3) The parameter of proportion gain is selected as $K_{p\lambda} = K_{Iv} K_{pi}$

Figure.6 illustrates a Bode diagram of the both the transfer functions. The figure shows that the system is very critical in shaping the Bode diagram of this disturbance rejection transfer function if the inrush current mitigation technique is integrated with controllers. This advantage benefits the power quality of the compensator output voltage. Analysis of the experimental results shows that the total harmonic distortion (THD) of load voltage without inrush current mitigation is 5.49% and with inrush current mitigation is 5.16%. The TABLE I summarizes the relationship between the error of fundamental component of load voltage and control gain $K_{I\lambda}$. The rejection ratio of the fundamental frequency can be increased by selecting a high control gain $K_{I\lambda}$.

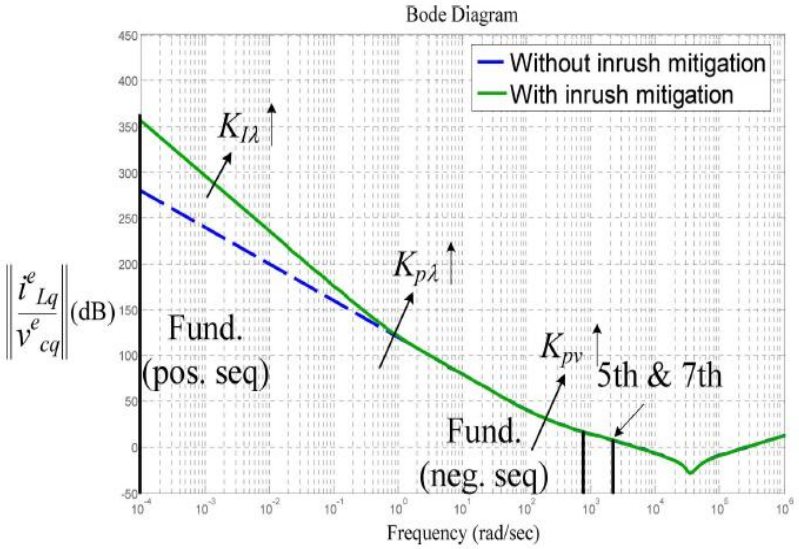

Fig.6 Comparison between conventional voltage–current state-feedback controller and the proposed inrush current mitigation technique integrated with state-feedback controller in disturbance rejection capability.

Table-1

$K_{I\lambda}$ gain	Error of fundamental component of the load voltage
Without inrush current mitigation technique	2.53%
$K_{I\lambda}$=100	1.18%
$K_{I\lambda}$=300	0.91%
$K_{I\lambda}$=1000	0.88%

V. SIMULINK MODEL AND RESULTS OF THE CONVENTIONAL SYSTEM

A. Without Inrush Mitigation Technique:

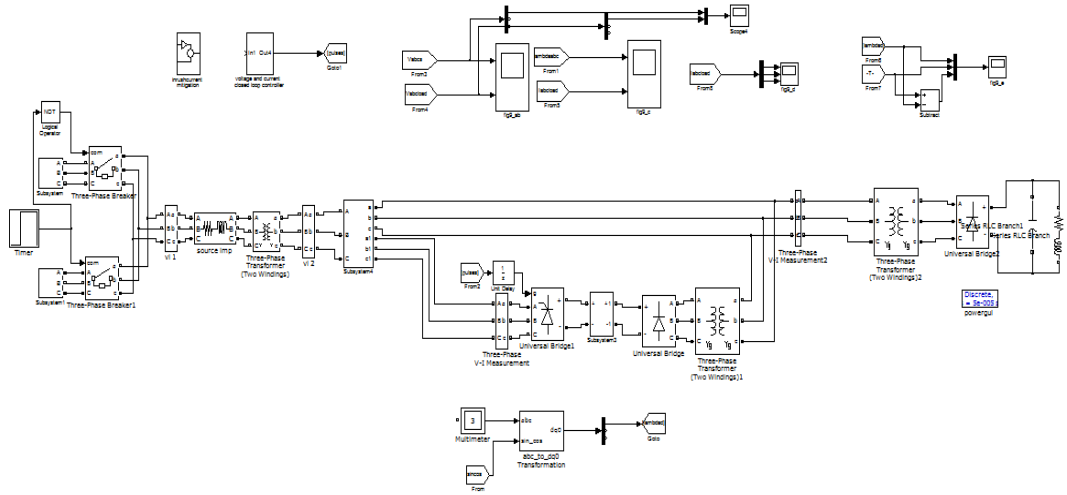

Fig.7 Simulink Block diagram for Without Inrush Mitigation Technique

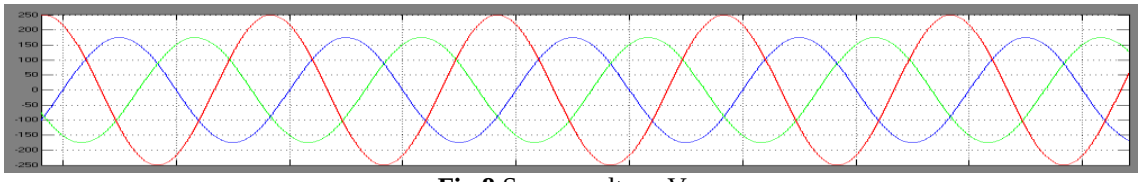

Fig 8 Source voltage V_s,

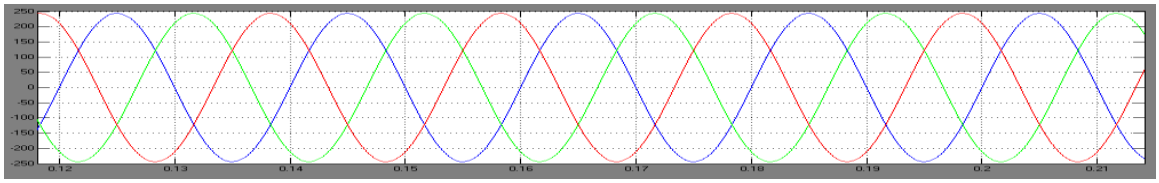

Fig.9 Load voltage $v_{l\text{-}l}$

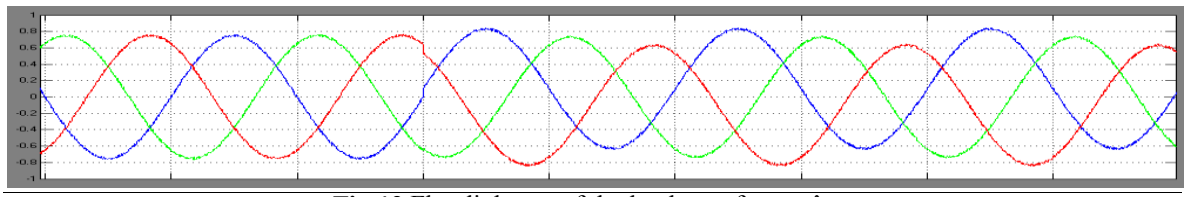

Fig.10 Flux linkages of the load transformer $\lambda_{L\text{-}L}$

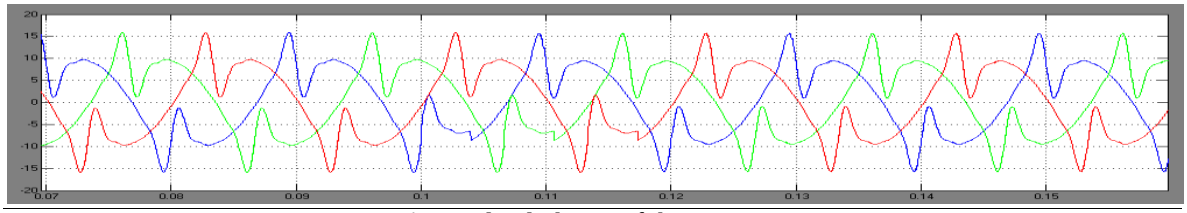

Fig.11 Flux linkages of the current I_L

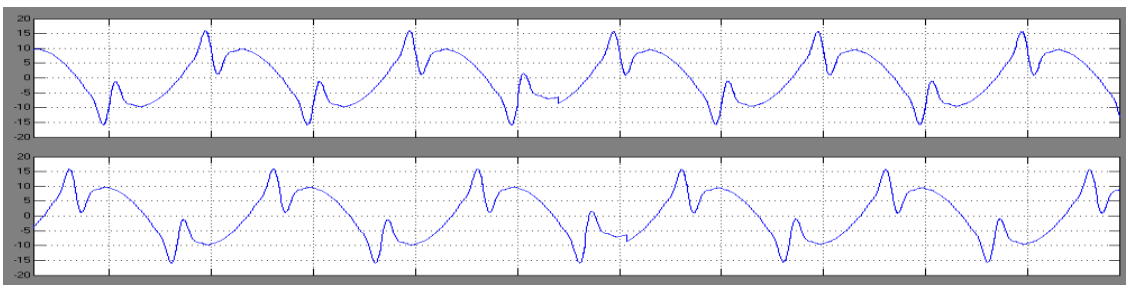

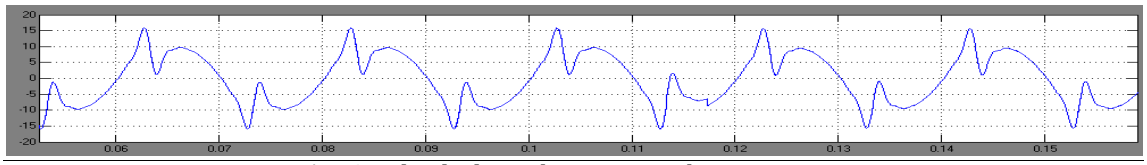

Fig 12 Individual inrush currents without mitigation

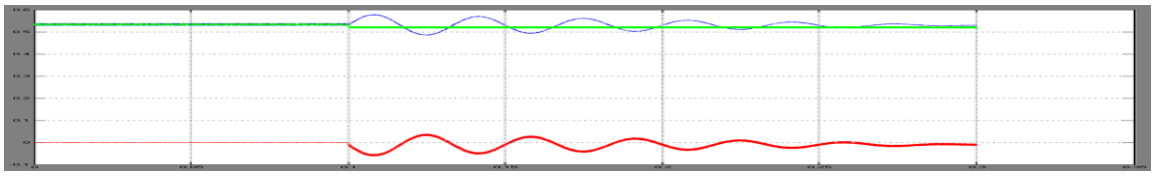

Fig 13 Flux linkage of d-axis λ^{e}_{L}

B. With Inrush Mitigation Technique:

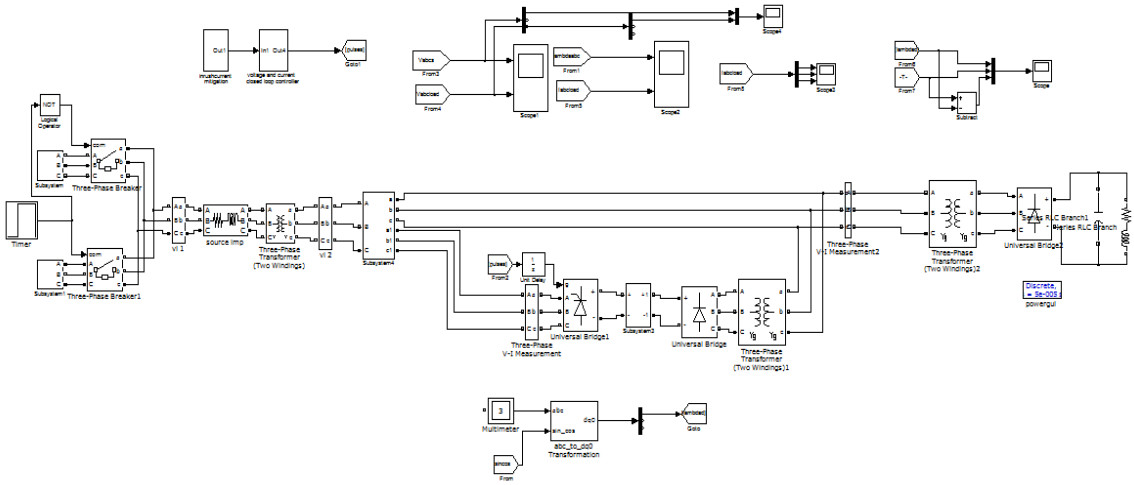

Fig 14 Block diagram for With Inrush Mitigation Technique

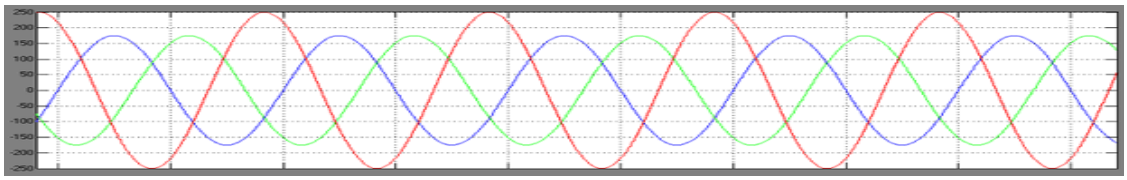

Fig 15 Source voltage V_s

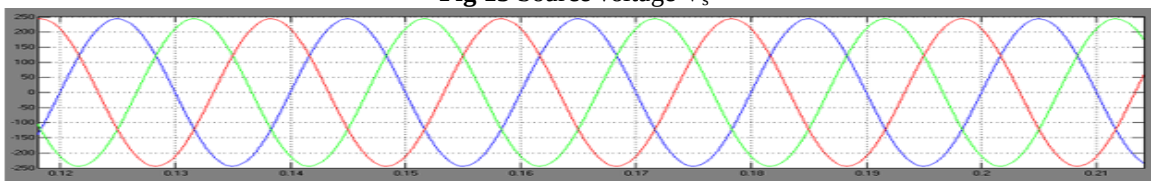

Fig 16 Load voltage $v_{l\text{-}l}$

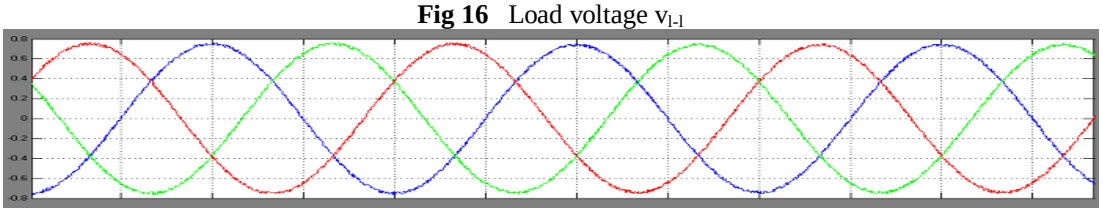

Fig 17 Flux linkages of the load transformer $\lambda_{L\text{-}L}$

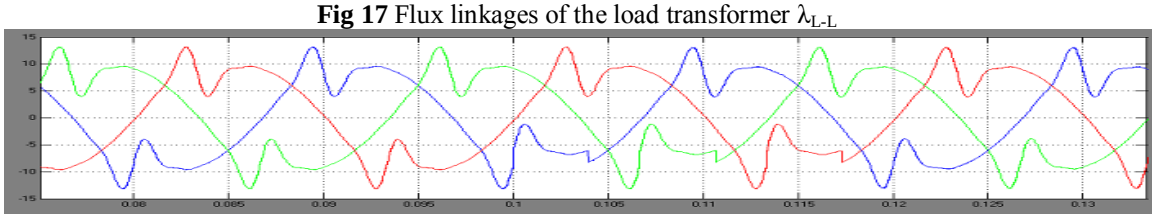

Fig 18 Flux linkages of the load current I_L

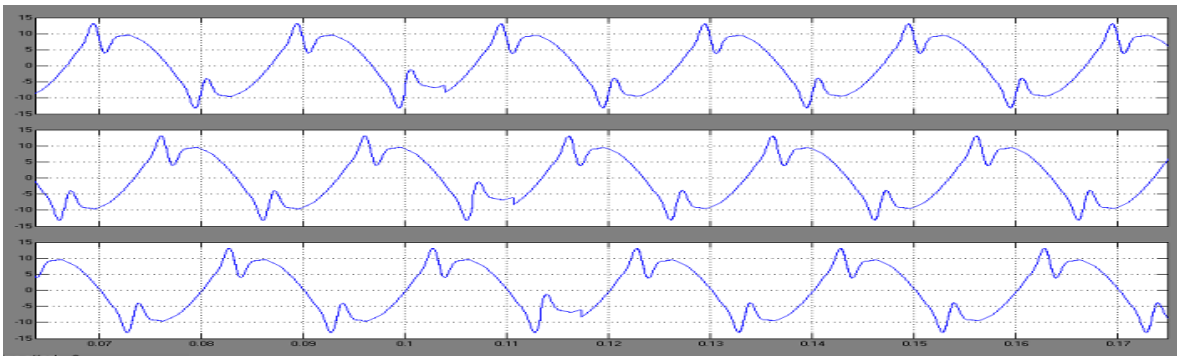

Fig 19 Individual inrush currents with mitigation

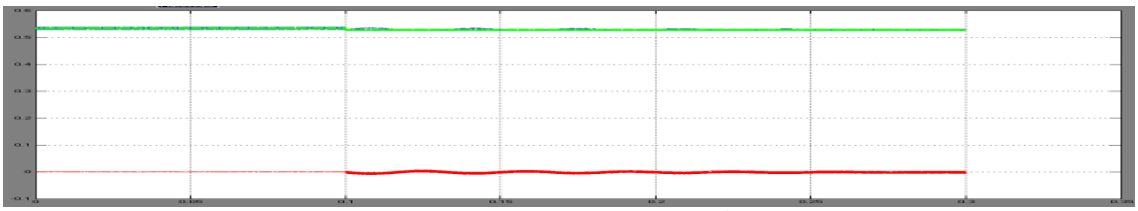

Fig 20 Flux linkage of d-axis λ^{e}_{L}

VI. CONCLUTION

In this paper, an active method of the series compensator used for reduction of inrush current during startup mode is proposed. Its main features are simple and effective control strategy for the reduction of transformer inrush current. This strategy on the basis of the current injection by series compensator is quite different from the conventional approaches. This control strategy is easy to implement because the series compensator is effective in reduction of the startup inrush current for all power-on angles without prior measurement on residual flux in a transformer core. Simulation results are presented to verify' the effectiveness of the proposed system for various operation parameters. The proposed system is simulated and the results demonstrate improvement in operating characteristics when compared with conventional approaches. It is shown that the proposed series compensator can suppress the inrush current effectively regardless of whether the transformer core has residual flux or not. Besides, the series compensator can inject compensation voltage to restore the load voltage to normal level for sensitive loads with fast response.

REFERENCES

[1] D. L. Brooks and D. D. Sabin, "An assessment of distribution system power quality," Elect. Power Res. Inst., Palo Alto, CA, EPRI Final Rep.TR-106249-V2, May 1996, vol. 2.

[2] W. E. Brumsickle, R. S. Schneider, G. A. Luckjiff, D. M. Divan, and M. F. McGranaghan, "Dynamic sag correctors: Cost-effective industrial power line conditioning," *IEEE Trans. Ind. Appl.*, vol. 37, no. 1, pp. 212–217, Jan./Feb. 2001.

[3] N. H. Woodley, "Field experience with dynamic voltage restorer (DVRTMMV) systems," in *Proc. IEEE Power Eng. Soc. Winter Meeting*, Jan. 23–27, 2000, vol. 4, pp. 2864–2871.

[4] R. Affolter and B. Connell, "Experience with a dynamic voltage restorer for a critical manufacturing facility," in *Proc. IEEE Transmiss. Distrib. Conf. Expo.*, 2003, vol. 3, pp. 937–939.

[5] C. N.-M. Ho, H. S. H. Chung, and K. T. K. Au, "Design and implementation of a fast dynamic control scheme for capacitor-supported dynamic voltage restorers," *IEEE Trans. Power Electron.*, vol. 23, no. 1, pp. 237–251, Jan. 2008.

[6] C. Meyer, R. W. De Doncker, Y. W. Li, and F. Blaabjerg, "Optimized control strategy for a medium-voltage DVR—Theoretical investigations and experimental results," *IEEE Trans. Power Electron.*, vol. 23, no. 6, pp. 2746–2754, Nov. 2008.

[7] J. G. Nielsen and F. Blaabjerg, "A detailed comparison of system topologies for dynamic voltage restorers," *IEEE Trans. Ind. Appl.*, vol. 41, no. 5, pp. 1272–1280, Sep./Oct. 2005.

[8] M. S. J. Asghar, "Elimination of inrush current of transformers and distribution lines," in *Proc. IEEE Power Electron., Drives Energy Syst. Ind. Growth*, 1996, vol. 2, pp. 976–980.

[9] Y. Cui, S. G. Abdulsalam, S. Chen, and W. Xu, "A sequential phase energization technique for transformer inrush current reduction—Part I: Simulation and experimental results," *IEEE Trans. Power Del.*, vol. 20, no. 2, pp. 943–949, Apr. 2005.

[10] W. Xu, S. G. Abdulsalam, Y. Cui, and X. Liu, "A sequential phase energization technique for transformer inrush current reduction—Part II: Theoretical analysis and design guide," *IEEE Trans. Power Del.*, vol. 20, no. 2, pp. 950–957, Apr. 2005.

[11] P. C. Y. Ling and A. Basak, "Investigation ofmagnetizing inrush current in a single-phase transformer," *IEEE Trans.Magn.*, vol. 24, no. 6, pp. 3217– 3222, Nov. 1988.

[12] C. Fitzer, A. Arulampalam, M. Barnes, and R. Zurowski, "Mitigation of saturation in dynamic voltage restorer connection transformers," *IEEE Trans. Power Electron.*, vol. 17, no. 6, pp. 1058–1066, Nov. 2002.

[13] G. Zenginobuz, I. Cadirci, M. Erims, and C. Barlak, "Performance optimization of induction motors during voltage-controlled softstarting," *IEEE Trans. Energy Convers.*, vol. 19, no. 2, pp. 278–288, Jun. 2004.

[14] J. Nevelsteen and H. Aragon, "Starting of large motors-methods and economics," *IEEE Trans. Ind. Appl.*, vol. 25, no. 6, pp. 1012–1018, Nov./Dec. 1989.

[15] H. Yamada, E. Hiraki, and T. Tanaka, "A novel method of suppressing the inrush current of transformers using a series-connected voltage-source PWM converter," in *Proc. IEEE Power Electron. Drives Syst. PEDS 2005 Int. Conf.*, 2006, vol. 1, pp. 280–285.

[16] S. Martinez, M. Castro, R. Antoranz, and F. Aldana, "Off-line uninterruptible power supply with zero transfer time using integrated magnetics," *IEEE Trans. Ind. Electron.*, vol. 36, no. 3, pp. 441–445, Aug. 1989.

[17] C.-C. Yeh and M. D. Manjrekar, "A reconfigurable uninterruptible power supply system for multiple power quality applications," *IEEE Trans. Power Electron.*, vol. 22, no. 4, pp. 1361–1372, Jul. 2007.

[18] *IEEE Recommended Practice for the Design of Reliable Industrial and Commercial Power Systems*, IEEE Standard 493-2007, 2007.

[19] P. T. Cheng, J. M. Chen, and C. L. Ni, "Design of a state-feedback controller for series voltage sag compensators," *IEEE Trans. Ind. Appl.*, vol. 45, no. 1, pp. 260–267, Jan./Feb. 2009.

[20] J. G. Nielsen, M. Newman, H. Nielsen, and F. Blaabjerg, "Control and testing of a dynamic voltage restorer (DVR) at medium voltage level," *IEEE Trans. Power Electron.*, vol. 19, no. 3, pp. 806–813, May 2004.

[21] M. Vilathgamuwa, A. A. D. R. Perera, and S. S. Choi, "Performance improvement of the dynamic voltage restorer with closed-loop load voltage and current-mode control," *IEEE Trans. Power Electron.*, vol. 17, no. 5, pp. 824–834, Sep. 2002.

[22] M. J. Ryan, W. E. Brumsickle, and R. D. Lorenz, "Control topology options for single-phase UPS inverters," *IEEE Trans. Ind. Appl.*, vol. 33, no. 2, pp. 493–501, Mar./Apr. 1997.

[23] *Recommended Practice for Voltage Sag and Interruption Ride-Through Testing for End-Use Electrical Equipment Less Than 1,000 Volts*, IEEE IAS P1668 Voltage Sag Ride-through Working Group, Dec. 2004.

[24] P. T. Cheng, W. T. Chen, Y. H. Chen, C. L. Ni, and J. Lin, "A transformer inrush mitigation method for series Voltage sag compensators," *IEEE Trans. Power Electron.*, vol. 22, no. 5, pp. 1890–1899, Sep. 2007.

[25] Y. H. Chen, "Voltage sag ride-through solutions based on solid-state transfer switches and uninterruptible power supplie," Ph.D. dissertation, Dept. Electr. Eng., National Tsing Hua Univ., to be published in July 2010.